TLR signaling adapter BCAP regulates inflammatory to reparatory macrophage transition by promoting histone lactylation

Ricardo A. Irizarry-Caro[a,b,c], Margaret M. McDaniel[a,b,c], Garrett R. Overcast[a,b,c], Viral G. Jain[d], Ty Dale Troutman[e], and Chandrashekhar Pasare[b,c,f,1]

[a]Immunology Graduate Program, University of Texas Southwestern Medical Center, Dallas, TX 75390; [b]Division of Immunobiology, Cincinnati Children's Hospital Medical Center, Cincinnati, OH 45229; [c]Center for Inflammation and Tolerance, Cincinnati Children's Hospital Medical Center, Cincinnati, OH 45229; [d]Division of Neonatology, University of Alabama at Birmingham, Birmingham, AL 35233; [e]Department of Cellular and Molecular Medicine, University of California, San Diego, La Jolla, CA 92093; and [f]Department of Pediatrics, University of Cincinnati College of Medicine, Cincinnati, OH 45267

Edited by Katherine A. Fitzgerald, University of Massachusetts Medical School, Worcester, MA, and accepted by Editorial Board Member Carl F. Nathan October 7, 2020 (received for review May 15, 2020)

Macrophages respond to microbial ligands and various noxious cues by initiating an inflammatory response aimed at eliminating the original pathogenic insult. Transition of macrophages from a proinflammatory state to a reparative state, however, is vital for resolution of inflammation and return to homeostasis. The molecular players governing this transition remain poorly defined. Here, we find that the reparative macrophage transition is dictated by B-cell adapter for PI3K (BCAP). Mice harboring a macrophage-specific deletion of BCAP fail to recover from and succumb to dextran sulfate sodium-induced colitis due to prolonged intestinal inflammation and impaired tissue repair. Following microbial stimulation, gene expression in WT macrophages switches from an early inflammatory signature to a late reparative signature, a process that is hampered in BCAP-deficient macrophages. We find that absence of BCAP hinders inactivation of FOXO1 and GSK3β, which contributes to their enhanced inflammatory state. BCAP deficiency also results in defective aerobic glycolysis and reduced lactate production. This translates into reduced histone lactylation and decreased expression of reparative macrophage genes. Thus, our results reveal BCAP to be a critical cell-intrinsic switch that regulates transition of inflammatory macrophages to reparative macrophages by imprinting epigenetic changes.

histones | PIK3AP1 | FOXO1 | IL-12 | tissue repair

Macrophages are highly plastic cells of the innate immune system that can perform a wide range of functions to advance and resolve inflammation (1, 2). During infection, classically activated or inflammatory macrophages are vital for the initial sensing of pathogens, and mediate inflammation through the secretion of proinflammatory cytokines like TNF and IL-12, which are necessary for microbial killing (3–6). However, if left unchecked, this inflammation can lead to widespread damage of the surrounding tissues (3–6). Alternatively, activated or reparative macrophages are responsible for dampening this inflammatory response and are involved in tissue repair by inducing matrix deposition and fibrogenesis (4, 7–9). Reparative macrophages express molecules such as arginase-1 (ARG1) and Krüppel like factor-4 (KLF4), which aid in their function (7, 10, 11). ARG1 is an enzyme that can suppress the formation of nitric oxide and is necessary for providing metabolites essential for effective wound repair (10, 12). KLF4 is a transcription factor that sustains the reparative gene signature in macrophages by promoting the expression of ARG1 and other reparative genes, like CD206 (11, 13).

In recent years, the importance of modulating macrophage responses along the inflammatory-reparative spectrum has become clear with regards to multiple inflammatory diseases, including atherosclerosis, obesity, cancer, and colitis, where altered macrophage states are hallmarks of disease (2, 14–22). During inflammatory diseases, macrophages modulate their behavior based on the microenvironmental cues they sense, which can often perpetuate the physiological problem due to persistent inflammation (2, 14–22). However, during wound repair, macrophages alter their function to limit inflammation and instead focus on clearing debris and promoting effective wound healing (23). While many studies have investigated the inflammatory and reparative capacity of macrophages by using a forced polarization system (3, 10–13, 24), it is important to note that within a normal inflammatory response, macrophages can respond to different microenvironmental cues and modulate their behavior along this inflammatory spectrum (25). This means that a cell can participate sequentially in both the induction and the resolution of inflammation (25). In short, the conventional M1-M2 denomination of macrophage states is only representative of their behavioral extremes, and it is therefore important to discuss macrophage behavior in terms of their broad inflammatory and reparative states that reflect true biology (3, 5, 8, 24). Recent work has shed light into a novel epigenetic modification that can

Significance

Macrophages initiate inflammation to eliminate invading microbes. Following clearance of inflammatory stimuli, macrophages down-regulate inflammatory genes and express repair genes to protect host tissues from damage. Here, we find that the adaptor B-cell adapter for PI3K (BCAP) facilitates this transition of inflammatory macrophages to reparative macrophages. Absence of BCAP in macrophages limits the ability of mice to repair intestinal tissues following inflammatory damage. Following Toll-like receptor stimulation, macrophages undergo aerobic glycolysis that results in lactate production, a process compromised in BCAP-deficient macrophages. This lactate is incorporated into histone tails and is involved in reparative macrophage transition. We find defective lactate production by BCAP-deficient macrophages results in reduced histone lactylation and expression of tissue repair genes, thus blunting their reparative transition.

Author contributions: R.A.I.C., M.M.M., and C.P. designed research; R.A.I.C., M.M.M., G.R.O., and T.D.T. performed research; T.D.T. contributed new reagents/analytic tools; R.A.I.C., G.R.O., V.G.J., and C.P. analyzed data; and R.A.I.C., M.M.M., and C.P. wrote the paper.

The authors declare no competing interest.

This article is a PNAS Direct Submission. K.A.F. is a guest editor invited by the Editorial Board.

[1]To whom correspondence may be addressed. Email: Chandrashekhar.Pasare@cchmc.org.

This article contains supporting information online at https://www.pnas.org/lookup/suppl/doi:10.1073/pnas.2009778117/-/DCSupplemental.

First published November 16, 2020.

modulate macrophage transition. It was shown that inflammatory macrophages undergo a novel histone modification, referred to as histone lactylation, which is dependent on aerobic glycolysis following M1 polarizing conditions (26). This modification allowed macrophages to up-regulate tissue repair signature following inflammatory stimulus. However, despite understanding the importance of macrophage transition between different states, the molecular events and players determining this response have yet to be elucidated.

Macrophages express a diverse set of pattern recognition receptors (PRRs) that allow them to detect various infectious insults and mount an appropriate inflammatory response (27). Stimulation of these PRRs, such as Toll-like receptors (TLRs), lead to macrophage activation and the production of proinflammatory, NF-κB– and AP1-dependent cytokines like TNF, IL-6, and IL-12 (27, 28). These cytokines play a major role in recruiting other innate cells to the site of infection and eventually destroying the pathogenic insult. During TLR signaling, multiple adapters and kinases coordinate the signaling cascade that culminates in induction of inflammatory effectors. Numerous proteins, such as A20, IL-1 receptor-associated kinase (IRAK)-M and single immunoglobulin IL-1R–related molecule (SIGIRR) have evolved to regulate TLR signaling by inhibiting interaction of adapters and kinases, thereby offsetting potentially damaging effects of prolonged cytokine production (29–32). Another important signaling event downstream of TLR engagement is the tandem activation of the PI3K-AKT pathway (33–35). The PI3K-AKT axis is known to be important in many cell types as its engagement promotes cell survival, proliferation, and protein synthesis (36). Following TLR ligation, PI3K phosphorylates and activates AKT, which plays a role in subsequently negatively regulating inflammatory responses by phosphorylating target proteins like glycogen synthase kinase 3β (GSK3β) and forkhead box protein O1 (FOXO1) (34, 35, 37, 38). GSK3β regulates the inflammatory response by differentially affecting the nuclear amounts of transcription factors NF-κB subunit p65 and CREB interacting with the coactivator CBP (37). FOXO1 is a transcriptional regulator of the *Tlr4* gene and helps promote NF-κB transcription of inflammatory effectors (38).

We previously identified a novel TLR signaling adapter called B-cell adapter for PI3K (BCAP) that mediates the activation of the PI3K-AKT pathway following TLR ligation (39–41). Importantly, the absence of BCAP led to exaggerated inflammatory responses after TLR activation, demonstrating that BCAP plays a critical role in the negative regulation of inflammation (39–41). The exaggerated inflammatory responses in BCAP-deficient macrophages were not due to enhanced activation of either NF-κB or MAP kinases, as these were unaltered. This suggested that BCAP could be modulating other effectors that regulate macrophage behavior following an inflammatory stimulus. As BCAP plays a central role in linking TLR signaling to the PI3K-AKT pathway, we hypothesized that BCAP might play an important role in modulating macrophage behavior that extends beyond regulating inflammatory cytokine production. Using both in vivo and in vitro approaches, we found that macrophage-intrinsic BCAP is responsible for coordinating the transition of macrophages from an inflammatory state to a reparative state, henceforth referred to as reparative macrophage transition, by dampening inflammation and up-regulating homeostatic/tissue repair genes. We identified two distinct phases of this transition. The first phase is defined by TLR engagement and NF-κB activation, culminating in the production of inflammatory effectors. During this phase, engagement of the PI3K-AKT pathway leads to inactivation of both FOXO1 and GSK3β resulting in the down-regulation of NF-κB targets (37, 38). In the second phase, macrophages undergo metabolic reprogramming that results in aerobic glycolysis, which is necessary for the production of lactate (42–44). The accumulation of lactate is used by the cell to efficiently promote reparative macrophage transition via the induction of histone lactylation (26). We find that in the absence of BCAP, macrophages do not engage the PI3K-AKT-FOXO1-GSK3β axis, which renders them hyperinflammatory. Abrogation of the PI3K-AKT pathway reduced aerobic glycolysis in BCAP-deficient macrophages, which resulted in decreased lactate production and defective histone lactylation, ultimately leading to impaired expression of tissue-repair genes. In mice that lack BCAP specifically in macrophages, this translates into compromised tissue repair following dextran sulfate sodium (DSS)-induced inflammatory colitis. These results suggest that BCAP is a central regulator of macrophage behavior and acts as a critical cell-intrinsic switch for macrophages to transition from inflammatory state to reparative state, through metabolic reprograming and epigenetic imprinting.

Results

Macrophage-Intrinsic BCAP Regulates Intestinal Inflammation and Tissue Repair. We have previously shown that BCAP-deficient mice are more susceptible to DSS-induced colitis, marked by increased inflammation and tissue damage (39). Given the importance of macrophages in resolving inflammation and repairing tissue damage (7, 21), we hypothesized that macrophage-intrinsic BCAP could be a driver in this heightened susceptibility to colitis. To test this, we generated mice that lacked BCAP specifically in macrophages by breeding mice harboring the floxed allele of BCAP (45) to mice carrying a LyzM Cre promoter-driven transgene (46). This cross yielded littermates with macrophages sufficient ($BCAP^{fl/fl}$; $BCAP^{WT}$) or deficient ($BCAP^{fl/fl}$ × LyzM-Cre; $BCAP^{\Delta M\phi}$) for BCAP. Bone marrow-derived macrophages (BMDM) from $BCAP^{\Delta M\phi}$ mice showed efficient deletion of BCAP whereas BMDM from $BCAP^{WT}$ showed normal expression (*SI Appendix*, Fig. S1*A*). To investigate the role of macrophage-intrinsic BCAP in regulating intestinal inflammation, $BCAP^{\Delta M\Phi}$ and $BCAP^{WT}$ littermates were treated with 2.5% DSS ad libitum. We found that $BCAP^{\Delta M\phi}$ mice suffered from more severe weight loss, colon shortening, and widespread tissue pathology marked by crypt ablation and immune cell infiltration (Fig. 1 *A*–*C* and *SI Appendix*, Fig. S1*B*). These results confirm that deletion of BCAP specifically in macrophages led to similar DSS-induced colitis susceptibility, as was reported in the full-body BCAP-deficient mice (39), suggesting that macrophage-intrinsic BCAP is critical to reduce susceptibility to colonic inflammation and disease. During colitis, inflammation causes the recruitment of inflammatory monocytes and neutrophils and leads to further epithelial damage (47). We found that $BCAP^{\Delta M\Phi}$ mice displayed increased recruitment and infiltration of inflammatory monocytes ($CD11b^{+}Ly6C^{Hi}Ly6G^{-}$) in the lamina propria (LP) (Fig. 1*D*). We also detected higher transcripts of the chemokine *Cxcl1* and neutrophil surface marker *Ly6g* (Fig. 1*E*) in the colonic tissues and higher neutrophilic infiltration in the LP (*SI Appendix*, Fig. S1*C*), suggesting that $BCAP^{\Delta M\phi}$ mice exhibited increased colonic inflammation following DSS treatment than their $BCAP^{WT}$ littermates.

Resolution of inflammation is a tightly coordinated process with an important contribution from reparative macrophages (21, 23, 47, 48). This process is characterized by sequential yet overlapping stages of acute inflammation followed by tissue repair that aims to restore tissue integrity and physiological function (21). To better understand the behavior of macrophages in this widespread colonic inflammation, we profiled tissue resident macrophages by flow cytometry. We found that the percentage of reparative macrophages ($CD11b^{+}CD206^{+}$) and expression of CD206 (*Mrc1*) were reduced in $BCAP^{\Delta M\phi}$ LP compared to $BCAP^{WT}$ (Fig. 1 *F* and *G*). These data suggest that absence of BCAP negatively affected the presence of reparative macrophages in the colonic tissue. Since reparative macrophages promote proper tissue repair following inflammatory damage, we asked

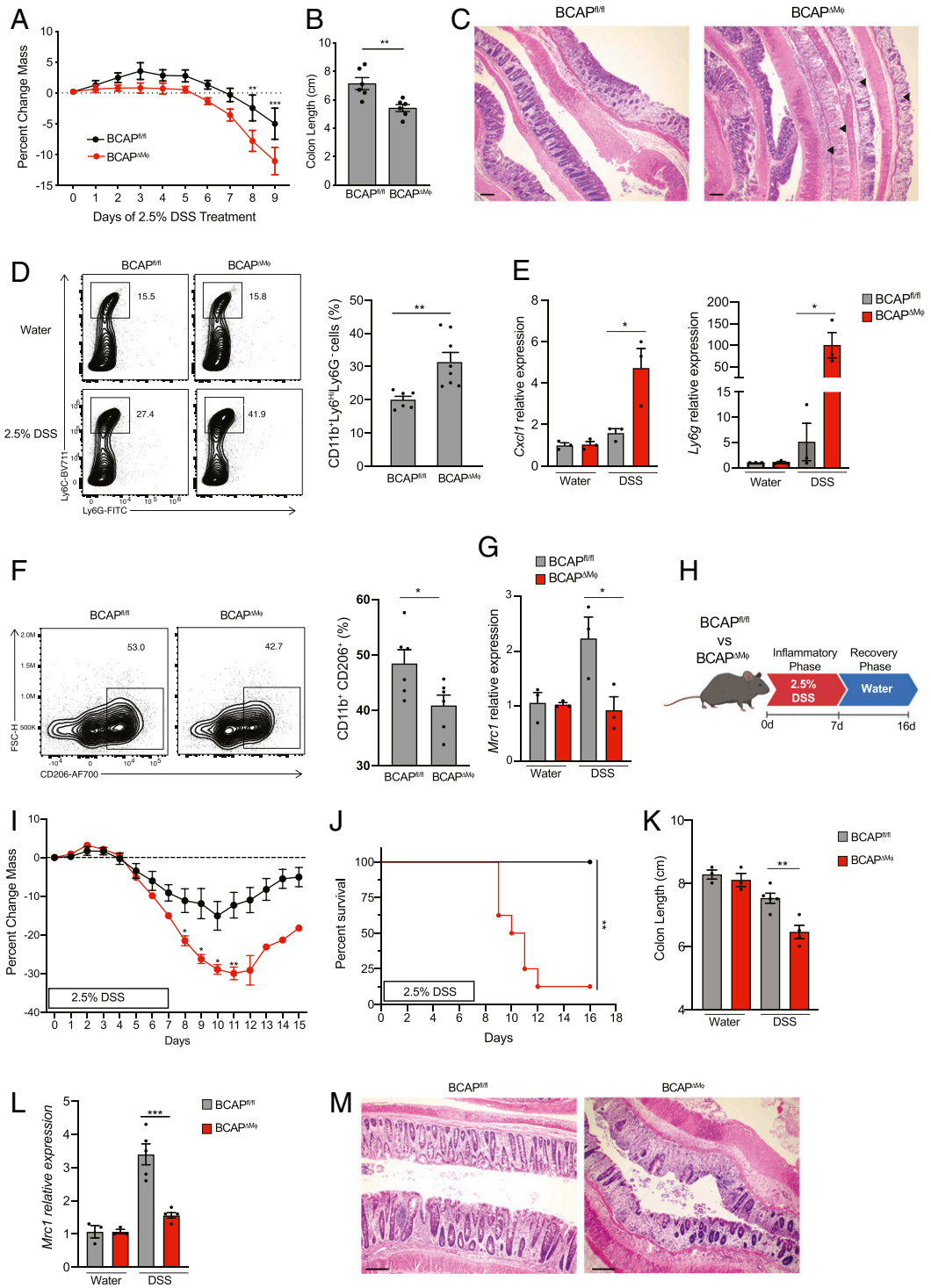

Fig. 1. Macrophage intrinsic BCAP regulates inflammation and repair response in vivo. (*A*) Weight loss of BCAP$^{fl/fl}$ and BCAP$^{\Delta M\phi}$ mice during 2.5% DSS treatment. (*B*) Mice from *A* were killed on day 9 and colons were measured from cecum to the rectum. (*C*) H&E stain of the colon from *B*. Arrowheads denote area of cell immune infiltration and crypt ablation. (Scale bar, 100 μm.) Data from *A*–*C* are representative of at least three independent experiments with $n =$ 6 per genotype. (*D*) Flow cytometry of LPLs isolated after 9 d of DSS treatment showing inflammatory monocytes (CD11b$^+$ Ly6C^{Hi} Ly6G$^-$). Representative plot (*Left*) with quantification (*Right*). (*E*) Expression of *Cxcl1* and *Ly6g* was measured by qPCR from colonic tissue after DSS treatment, normalized to *Hprt1*. (*F*) Flow cytometry of LPLs isolated after 9 d of DSS treatment showing reparative macrophages (CD11b$^+$ CD206$^+$). Representative plot (*Left*) with quantification (*Right*). (*G*) Expression of *Mrc1* (CD206) measured by qPCR from colonic tissue isolated from *F*, normalized to *Hprt1*. (*H*) Diagram of DSS repair model including 7 d of 2.5% DSS treatment followed with 9 d of water (made using Biorender). (*I*) Weight loss of BCAP$^{fl/fl}$ and BCAP$^{\Delta M\phi}$ mice during DSS and water treatment shown in *H*. (*J*) Survival curve of BCAP$^{fl/fl}$ and BCAP$^{\Delta M\phi}$ mice from *I*. (*K*) BCAP$^{fl/fl}$ and BCAP$^{\Delta M\phi}$ mice were killed before succumbing to disease and colons were measured from cecum to the rectum. (*L*) qPCR of *Mrc1* (CD206) from colonic tissue after DSS treatment, normalized to *Hprt1* ($n = 5$ per genotype). (*M*) H&E stain of the colon of BCAP$^{fl/fl}$ and BCAP$^{\Delta M\phi}$ mice from *K*. (Scale bar, 200 μm.) Data from *A*–*C* is $n = 6$ per genotype, *D* is BCAP$^{fl/fl}$ ($n = 6$) and BCAP$^{\Delta M\phi}$ ($n = 8$), *E* is $n = 3$ per genotype, *F* is $n = 6$ per genotype, *G* is $n = 3$ per genotype, *I*–*J* BCAP$^{fl/fl}$ ($n = 6$) and BCAP$^{\Delta M\phi}$ ($n = 8$), *K* is $n = 5$ per genotype. Error bars represent SEM and Student *t* test were performed in all graphs except survival. Survival statistics were calculated with log-rank test. *$P < 0.05$, **$P < 0.01$, ***$P < 0.001$.

if BCAP$^{\Delta M\phi}$ were able to recover from this colonic inflammation after the removal of DSS. We used an established model of intestinal tissue repair (49–51), where mice are treated with 2.5% DSS for 7 d followed by a recovery phase of 9 additional days (Fig. 1*H*). Using this model, we found that BCAP$^{\Delta M\phi}$ mice lost significantly more weight than their BCAP^{WT} littermates by day 8 and were unable to recover from this weight loss by day 15 (Fig. 1*I*). Furthermore, 85% of BCAP$^{\Delta M\phi}$ mice succumbed to disease by day 16 (Fig. 1*J*), suggesting that they were unable to resolve colonic inflammation. To further assess the resolution of intestinal inflammation, a cohort of mice were killed following a recovery phase of 4 d and colons were harvested. We found that surviving BCAP$^{\Delta M\phi}$ mice still exhibited colon shortening, whereas their littermate controls were able to recover from the DSS-induced damage when compared to a water treated control (Fig. 1*K*). Additionally, we detected lower levels of CD206 mRNA (*Mrc1*) in the colon of BCAP$^{\Delta M\phi}$ mice following the recovery phase (Fig. 1*L*). This was also true for other known repair genes, such as *Arg1* and *Klf4* (*SI Appendix*, Fig. S1*D*). This was further exemplified by the fact that BCAP$^{\Delta M\phi}$ mice were not able to repair their intestinal crypts during the recovery phase, as suggested by histology (Fig. 1*M* and *SI Appendix*, Fig. S1*E*). Overall, these data suggest that BCAP expression in macrophages is critical for resolving tissue damage following DSS-induced colitis. There is large body of evidence that inflammatory macrophages transition to reparative state to aid in tissue repair and wound healing, and these data suggest that macrophage-intrinsic BCAP might be playing a critical role in this transition.

Absence of BCAP Leads to Defective Transition of Macrophages from an Inflammatory to Reparative State. To gain mechanistic insight into BCAP-regulated reparative transition, we next sought to model this reparative macrophage transition process in vitro. We hypothesized that a pulse of TLR stimuli triggering NF-κB activation would lead to the up-regulation of inflammatory effectors, but that this inflammation would be resolved following removal or clearance of the ligand. We generated BMDMs from WT mice and pulsed them with LPS for 3 h, washed off excess ligand thoroughly, then assessed how gene transcription changed over time (Fig. 2*A*). Immediately following the LPS pulse, WT BMDMs up-regulated the inflammatory cytokine *Il12b*, as expected (Fig. 2*B*). However, following the removal of LPS, production of *Il12b* waned over time (Fig. 2*B*). Mirroring this down-regulation of inflammatory cytokine, WT BMDMs began to up-regulate reparative genes, such as *Arg1*, *Klf4*, and *Mmp9* (Fig. 2*C* and *SI Appendix*, Fig. S2*A*). The transition of gene-expression phenocopies in vivo macrophage behavior observed in our DSS model (Fig. 1*L*), albeit on a longer time scale. Heat-killed (HK) *Escherichia coli* was also used to assess this inflammatory-to-reparative macrophage transition as it activates a broad range of TLRs and PRRs, and does not require washing to remove ligand as bacteria are naturally cleared by the macrophages by phagocytosis (Fig. 2*A*) (52, 53). Again, we found a similar bimodal trend where BMDMs first up-regulate inflammatory genes, then switch to reparative genes (Fig. 2 *D* and *E*).

Given our previous finding that BCAP is necessary to limit inflammation downstream of TLR signaling via the engagement of the PI3K-AKT pathway (39–41), we then asked how BCAP$^{-/-}$ BMDMs would respond to this in vitro inflammatory pulse. Absence of BCAP does not affect the ability of bone marrow precursors to differentiate into macrophages (*SI Appendix*, Fig. S2*B*). However, consistent with our previous results, we found that BCAP$^{-/-}$ BMDMs produced more IL-12 at both the transcript and protein level following the 3-h LPS pulse than WT BMDMs (Fig. 2*C* and *SI Appendix*, Fig. S2*C*). Furthermore, BCAP$^{-/-}$ BMDMs exhibited sustained production of inflammatory cytokines, as they were still producing *Il12b* transcript following 24 h of LPS removal (Fig. 2*B*). While WT BMDMs were able to up-regulate reparative genes following removal of LPS, we found that BCAP$^{-/-}$ BMDMs were deficient in this reparative transition as they produced significantly less *Arg1*, *Klf4*, and *Mmp9* after 24 and 48 h of LPS removal (Fig. 2*C* and *SI Appendix*, Fig. S2*A*). We again used HK *E. coli* to assess this reparative transition in BCAP$^{-/-}$ BMDMs and found a similar trend as before, where BCAP$^{-/-}$ BMDMs had an enhanced and sustained production of *Il12b* over time and failed to efficiently up-regulate reparative genes *Arg1* and *Klf4* (Fig. 2 *D* and *E*). Taken together, these in vitro data suggest that macrophage-intrinsic BCAP indeed plays a critical role in reparative macrophage transition following various inflammatory stimuli.

Lack of Inactivation of FOXO1 and GSK3β Contributes to Higher Inflammatory Responses of BCAP-Deficient Macrophages. To further understand the molecular mechanisms regulating this reparative macrophage transition, we decided to categorize the response of macrophages into two phases. The first phase (3-h pulse) was marked by BCAP$^{-/-}$ BMDMs having elevated inflammation as compared to WT BMDMs. The second phase (12 to 48 h following removal or clearance of ligand) was marked by the up-regulation of reparative genes by WT BMDMs, which was blunted in the BCAP$^{-/-}$ BMDMs. Immediately following TLR ligation, the PI3K-AKT pathway gets engaged whereby AKT phosphorylates and inactivates its targets GSK3β and FOXO1, thereby negatively regulating the production of further inflammatory mediators (37, 38). Following LPS stimulation of WT BMDMs, we indeed found induced phosphorylation of AKT, GSK3β, and FOXO1, suggesting that the proper negative regulators of TLR signaling were active in this system (Fig. 2*F*). BCAP$^{-/-}$ BMDMs stimulated for the same time showed significantly less phosphorylation of AKT, which translated into reduced phosphorylation of both FOXO1 and GSK3β, implying that these factors remain constitutively active (37, 38, 54, 55) and perpetuate a hyperinflammatory response (Fig. 2*F*).

If sustained activation of GSK3β and FOXO1 in BCAP$^{-/-}$ BMDMs are responsible for the hyperinflammation seen in the inflammatory phase of the reparative transition, we hypothesized that specific inhibition of GSK3β or FOXO1 might return the inflammatory response of BCAP$^{-/-}$ BMDMs back to WT levels. BCAP$^{-/-}$ BMDMs were pretreated with SB216763 (GSK3βi) or AS1842856 (FOXO1i) and pulsed with LPS as before (Fig. 2*A*). Acute inhibition of GSK3β and FOXO1 drastically reduced the production of IL-12 and IL-6 by BCAP$^{-/-}$ BMDMs without greatly affecting the WT BMDMs (Fig. 2*G*). This same trend was observed when BCAP$^{-/-}$ BMDMs were pretreated with lithium chloride (LiCl), another GSK3β inhibitor (56) (*SI Appendix*, Fig. S2*D*). Taken together, these data suggest that BCAP dampens the inflammatory phase of macrophage response by engaging the PI3K-AKT pathway and inactivating FOXO1 and GSK3β.

We next asked if by limiting the inflammatory phase of BCAP$^{-/-}$ BMDMs, we had rescued their ability to undergo the reparative macrophage transition described in Fig. 2*A*. We again pretreated BCAP$^{-/-}$ and WT BMDMs with the specific inhibitors and pulsed them with LPS for 3 h, as before (Fig. 2*A*). After removal of LPS, we assessed the ability of these cells to up-regulate reparative genes. Surprisingly, we found that while inhibition of GSK3β or FOXO1 prevented the elevated inflammation found in BCAP$^{-/-}$ BMDM (Fig. 2*G*), it did not rescue the failure of these BMDMs to sustain a reparative gene program (Fig. 2*H*). Taken together, these data suggest that while the heightened and sustained proinflammatory response found in BCAP$^{-/-}$ BMDMs is due to failure in engaging proper negative regulatory pathways, their defect in undergoing reparative transition is potentially a result of an independent mechanism.

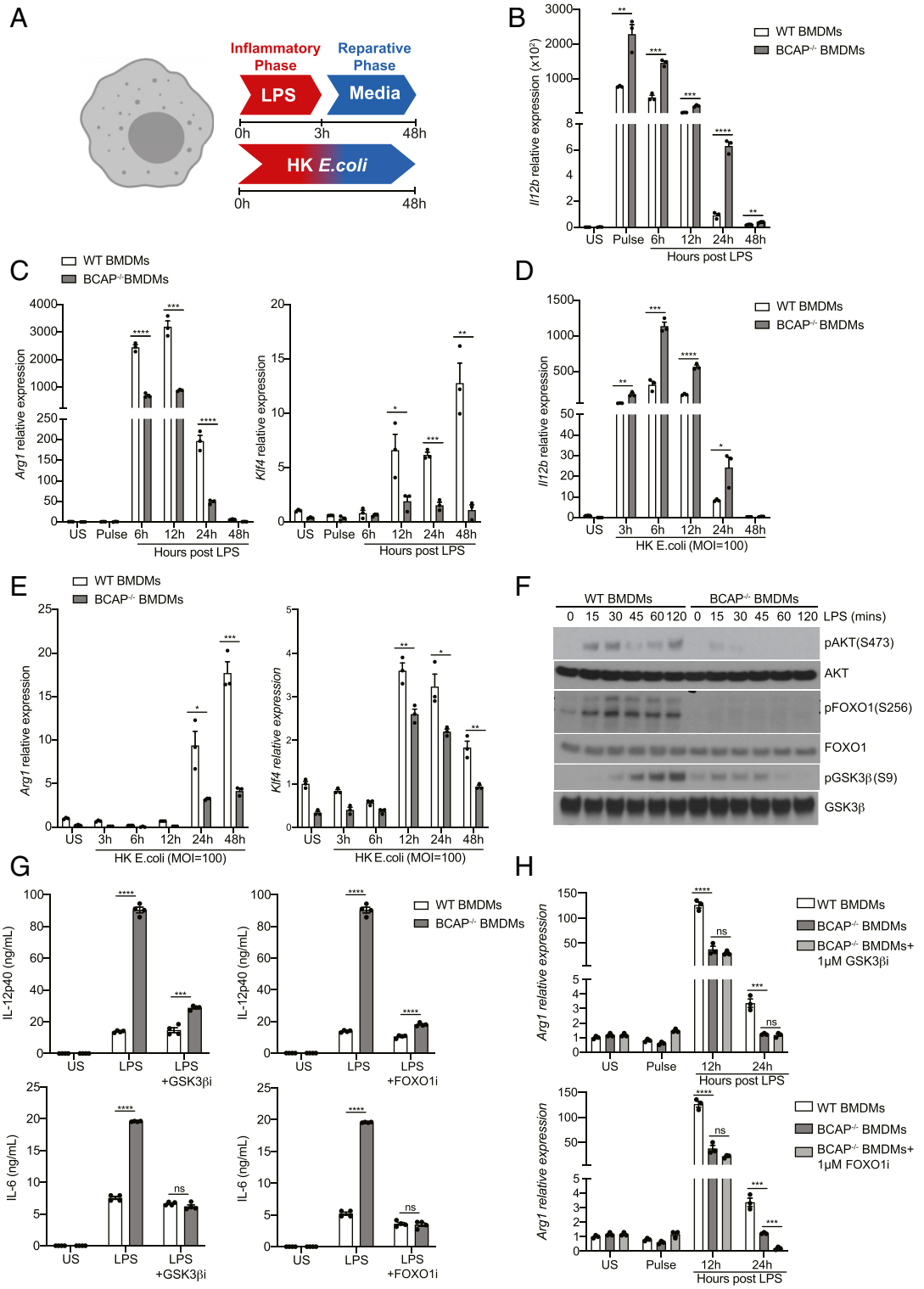

Fig. 2. BCAP modulates the transition of macrophages from an inflammatory to a reparative state. (*A*) Diagram of in vitro model of reparative macrophage transition. Briefly, BMDMs are pulsed with LPS (100 ng/mL) for 3 h (inflammatory phase), washed extensively, then cultured with fresh media for up to 48 h (reparative phase). BMDMs were also are stimulated with HK *E. coli* (MOI 100) up to 48 h (made using Biorender). (*B* and *C*) Expression of *Il12b* or *Arg1* and *Klf4* measured by qPCR from WT and BCAP$^{-/-}$ BMDMs subjected to LPS stimulation detailed in *A*, normalized to *Hprt1*. (*D* and *E*) Expression of *Il12b* or *Arg1* and *Klf4* measured by qPCR from WT and BCAP$^{-/-}$ BMDMs subjected to HK *E. coli* stimulation detailed in *A*, normalized to *Hprt1*. (*F*) Western blot of WT and BCAP$^{-/-}$ macrophages stimulated with LPS for the indicated time points. Cells were serum starved for 3 h prior to stimulation. (*G*) IL-12 and IL-6 were measured by ELISA in the supernatant from WT and BCAP$^{-/-}$ BMDMs stimulated with LPS for 3 h in the presence or absence of 1 μM GSK3b inhibitor (SB216763) or 1 μM FOXO1i (AS1842856). (*H*) Expression of *Arg1* measured by qPCR in WT and BCAP$^{-/-}$ BMDMs stimulated as detailed in *A* in the presence or absence of 1 μM GSK3β inhibitor (SB216763) or 1 μM FOXO1i (AS1842856). Normalized to *Hprt1*. (*B–E* and *H*) Data are representative of three independent experiments. (*F*) Data are representative of two independent experiments. Error bars represent SEM and Student *t* test was performed. *$P < 0.05$, **$P < 0.01$, ***$P < 0.001$, ****$P < 0.0001$.

BCAP Is Required for Optimal Glycolysis following Microbial Stimulation. Following TLR activation, macrophages shift their metabolism to meet energy requirements necessary to support the production of inflammatory mediators (43, 44, 57). The switch from oxidative phosphorylation to aerobic glycolysis (42–44) is a hallmark of this metabolic shift following TLR ligation (43, 44). Due to the essential role of BCAP in linking TLRs to the PI3K-AKT pathway, we hypothesized that BCAP-deficient macrophages may have a defect in their metabolic reprograming, thereby affecting the reparative macrophage transition. To test this hypothesis, we pulsed WT and BCAP$^{-/-}$ BMDMs with HK *E. coli* or LPS for 3 h, as described previously (Fig. 2*A*). We then measured the extracellular acidification rate (ECAR) at the indicated time points using glycolysis stress test on the Seahorse platform. We found that following removal of LPS for 12 or 24 h, BCAP$^{-/-}$ BMDMs had significantly decreased ECAR when compared to WT BMDMs, suggesting that they underwent reduced glycolysis (Fig. 3 *A* and *B*). We further found that BCAP$^{-/-}$ BMDMs also had significantly less glycolytic reserve as compared to WT BMDMs (Fig. 3*C*). BMDM stimulation with HK *E. coli* led to similar results where BCAP$^{-/-}$ BMDMs had consistently less ECAR and displayed reduced glycolysis (*SI Appendix*, Fig. S3). Of note, BCAP$^{-/-}$ BMDMs exhibited lower ECAR even when not actively stimulated with TLR ligands, suggesting the possibility that there is some tonic TLR signaling that contributes to BCAP-dependent basal ECAR. To further assess the impairment in induced glycolysis, we examined the expression of key glycolytic enzymes following LPS pulse.

Consistent with ECAR data, BCAP$^{-/-}$ BMDMs exhibited decreased expression of hexokinase-2 (*Hk2*) and lactate dehydrogenase A (*Ldha*), two key mediators of glycolysis (58–60) (Fig. 3*D*). In correlation with reduced *Ldha* expression, BCAP$^{-/-}$ BMDMs produced significantly less lactate than WT BMDMs following 12 and 24 h of LPS removal (Fig. 3*E*). Taken together, these data show that BCAP contributes to the metabolic reprogramming of macrophages following TLR ligation, specifically by enhancing glycolysis and lactate production. Studies have shown that metabolic reprogramming toward aerobic glycolysis is necessary to support macrophage functions, including secretion of inflammatory cytokines and phagocytosis (43, 44, 57, 61). Perplexingly, BCAP-deficient macrophages secrete more inflammatory cytokines despite defective glycolysis, suggesting a prominent role for GSK3β and FOXO1 in their contribution to the inflammatory phenotype. This prompted us to further examine if defective glycolysis affected the transition of BCAP deficient macrophages to a reparative state.

BCAP Promotes Reparative Macrophage Transition through Histone Lactylation. In addition to providing fuel for the cell, glycolysis leads to the production of metabolites that can also directly participate in signaling and modify transcriptional responses of cells (62–64). An example of this during glycolysis is the byproduct lactate, which has been suggested to act as an essential component of carbon metabolism. Recent studies have also suggested that lactate can modulate macrophage behavior directly by participating in histone modifications (26). This novel epigenetic modification, referred to as histone lactylation, was shown to mediate the transcriptional up-regulation of certain loci associated with reparative macrophages (26). Inhibition of glycolysis using 2-DG was shown to abrogate histone lacytlation, as it prevented the cell from producing appropriate lactate (26). Since histone lactylation is dependent on the ability of the cell to produce lactate, we hypothesized that the defect in BCAP$^{-/-}$ BMDMs to undergo reparative macrophage transition could be due to their defect in glycolytic capacity and the decreased lactate accumulation following inflammatory stimuli.

To test this hypothesis, we again pulsed WT and BCAP$^{-/-}$ BMDM with HK *E. coli* or LPS for 3 h, as described above (Fig. 2*A*). After 12 to 24 h of LPS removal, we isolated histones from WT and BCAP$^{-/-}$ BMDMs and measured histone lactylation via Western blot. We found that BCAP was required for macrophages to efficiently lactylate histones following LPS pulse (Fig. 4*A* and *SI Appendix*, Fig. S4). This correlates with our previous result that WT BMDMs were able to produce more lactate than BCAP$^{-/-}$ BMDMs in response to TLR ligation (Fig. 3*E*). Addition of exogenous sodium lactate (NaLa) promotes histone lactylation (26), and we found that BCAP$^{-/-}$ BMDMs were indeed able to rescue histone lactylation following culture with NaLa (Fig. 4*A*). Finally, we asked if adding NaLa and enhancing histone lactylation was able to rescue the defect of BCAP$^{-/-}$ BMDMs to undergo reparative macrophage transition. We monitored reparative gene expression following 12 to 48 h of LPS removal in the presence of NaLa and found that BCAP$^{-/-}$ BMDM were now able to up-regulate their expression of *Arg1* to a comparable level as WT BMDMs by 12 h, and *Klf4* by 48 h (Fig. 4*B*). In response to stimulation with HK *E. coli*, BCAP$^{-/-}$ BMDMs were similarly unable to efficiently lactylate histones or up-regulate reparative macrophage genes (Fig. 4 *C* and *D*), but this can be rescued by the addition of NaLa. These data reveal that BCAP is the upstream adapter linking TLR signaling to optimal aerobic glycolysis in macrophages and the resulting lactate is necessary for proper histone lactylation that promotes expression of reparative genes, and thus reparative macrophage transition.

Discussion

The ability of macrophages to undergo a reparative transition is essential for the resolution of inflammation and tissue repair following damage (7, 25). Our study has revealed that this reparative macrophage transition can occur sequentially following the removal of inflammatory stimuli, and without exogenous signals. Importantly, we identified BCAP as a critical regulator of this transition, as it activates a negative feedback arm of TLR signaling, namely PI3K-AKT. In the absence of BCAP, macrophages respond to TLR ligands with a heightened and sustained inflammatory response, and do not up-regulate genes associated with reparative transition. This defect plays a major role during colonic inflammation, as the inability to undergo reparative transition leads to worsened inflammatory disease, inability to repair tissue damage, and eventual mortality.

Macrophages rely on PRRs, like TLRs, to mount an appropriate innate immune response following pathogenic insult. Many aspects of TLR signaling and how it affects macrophage behavior have been studied throughout the years (3, 27). As the overarching consequence of TLR ligation is the activation of NF-κB and AP-1, many of these behavior modifications stem from these transcription factors. Enhanced phagocytosis and production of inflammatory cytokines and chemokines are among the most well-studied features of macrophage activation downstream of TLR signaling (27, 53, 65, 66). In addition to induction of inflammatory effectors, TLR signaling also induces metabolic changes within the cells. In macrophages and dendritic cells, a switch from oxidative phosphorylation to glycolysis is thought to be necessary in supporting the increased demand for physiological processes like production and secretion of cytokines (43, 57, 59, 61, 67). Interestingly, we have found that while BCAP$^{-/-}$ macrophages exhibit enhanced inflammatory responses, they exhibit decreased glycolysis and glycolytic capacity following LPS and HK *E. coli* stimulation. This reduction in glycolysis seen in BCAP$^{-/-}$ macrophages is likely due to their intrinsic defect in engaging the PI3K-AKT pathway, which is necessary for the glycolytic switch following macrophage activation (43, 59). The mechanism by which BCAP$^{-/-}$ macrophages provide energy for sustaining high inflammation remains unclear. Previous studies

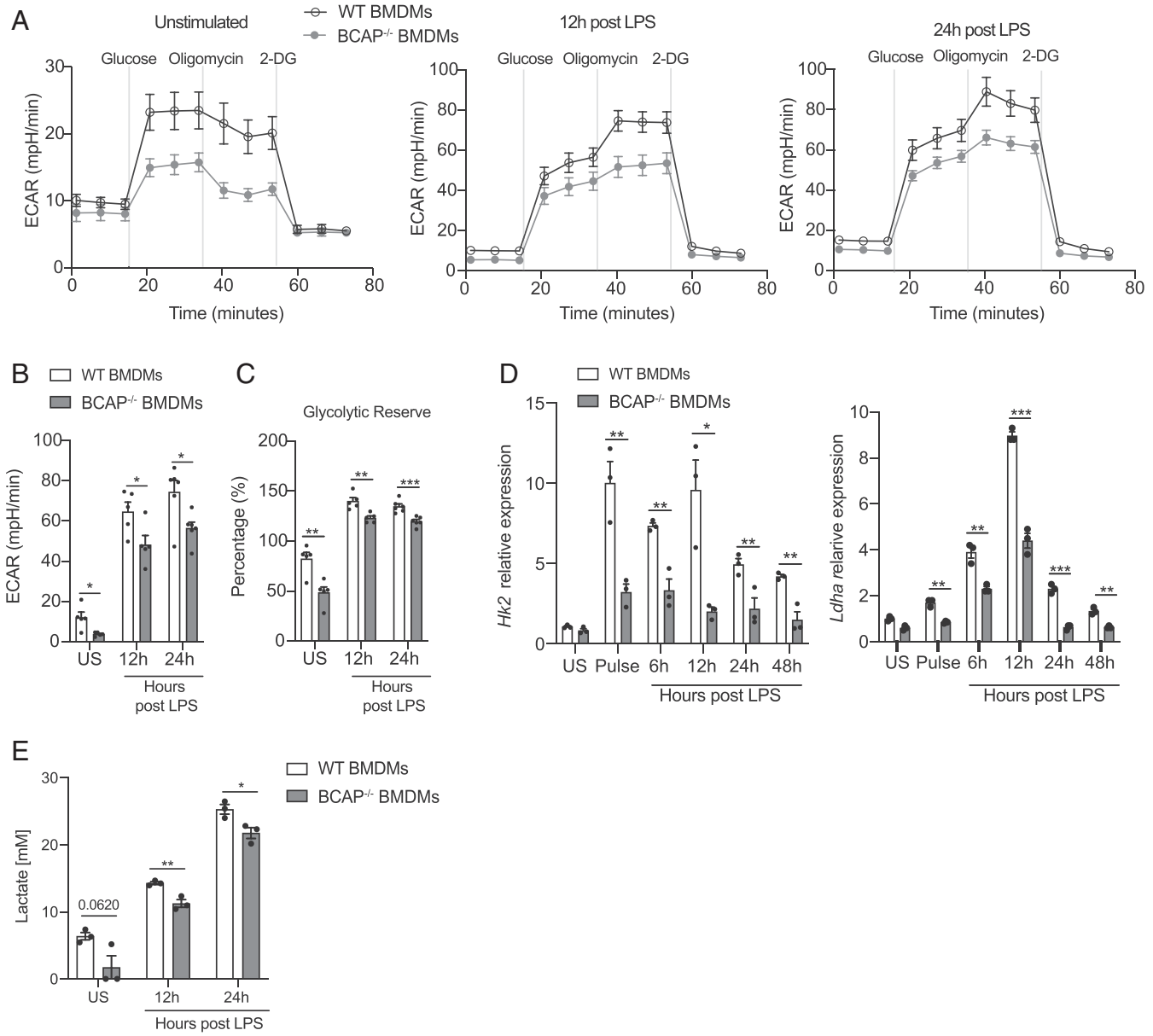

Fig. 3. BCAP modulates glycolytic reprograming of macrophages after LPS stimulation. (*A*) ECAR response from WT or BCAP$^{-/-}$ BMDMs stimulated with LPS (100 ng/mL) for 3 h then removed for indicated time. Representative of three independent experiments. (*B*) Measurement of ECAR indicating glycolytic capacity and (*C*) glycolytic reserve from *A*. (*D*) Expression of *Hk2* and *Ldha* measured by qPCR from WT or BCAP$^{-/-}$ BMDMs stimulated with LPS as described in Fig. 2*A*. Normalized to *Hprt1*. (*E*) Lactate production from WT or BCAP$^{-/-}$ BMDMs stimulated with LPS as described in Fig. 2*A*. (*A–C* and *E*) $n = 3$ to 6 biological replicates. (*D*) Data are representative of three independent experiments. Error bars represent SEM and Student *t* test was performed. *$P < 0.05$, **$P < 0.01$, ***$P < 0.001$.

have shown that in the absence of glycolysis, macrophages can meet their energetic demand through fatty acid synthesis (68–70). We expect that these BCAP$^{-/-}$ macrophages might have similarly adopted the fatty acid synthesis method for supporting their enhanced quantities of inflammatory cytokines.

It has now been well documented that metabolites are able to modulate transcriptional responses at diverse levels including epigenetic modifications (42, 63, 64). Previous research found that macrophages undergo a novel epigenetic modification that relies on metabolic reprogramming following inflammatory stimulus (26). This modification relied on aerobic glycolysis following canonical-M1 polarizing conditions (IFN-γ+LPS), which led to increased levels of lactate, thus promoting histone lactylation and the selective up-regulation of reparative genes (26). In this study, we find that BCAP is required for efficient histone lactylation during macrophage-intrinsic reparative transition. This is likely because BCAP$^{-/-}$ macrophages had decreased expression of key glycolytic enzymes like *Hk2* and *Ldha*, which is correlated with reduced production of lactate after TLR ligation. Due to this decreased production of lactate, BCAP$^{-/-}$ macrophages exhibited less histone lactylation than WT macrophages and were unable to effectively up-regulate reparative genes. Interestingly, by providing exogenous lactate in the form of NaLa, we were able to rescue both inducible histone lactylation and reparative transition of BCAP-deficient macrophages. Our data therefore agree that metabolites, such as lactate, can dampen macrophage inflammation specifically during reparative macrophage transition. Of note, there appears to be a differential

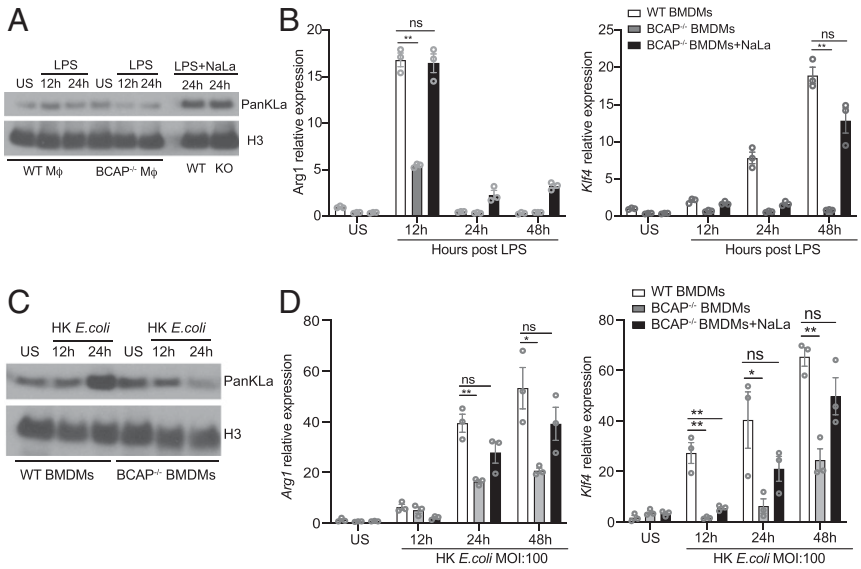

Fig. 4. BCAP promotes reparative macrophage transition through histone lactylation. (*A*) Histone pan lysine lactylation (panKla) was measured in WT or BCAP$^{-/-}$ BMDMs, by Western blotting, following stimulation with LPS as detailed in Fig. 2*A*. (*B*) Expression of *Arg1* and *Klf4* was measured by qPCR from WT or BCAP$^{-/-}$ BMDMs treated as in *A* in the presence or absence of 25 mM NaLa. Normalized to *Hprt1*. (*C*) Histone pan lysine lactylation (panKla) was measured in WT or BCAP$^{-/-}$ BMDMs, by Western blotting, following stimulation with HK *E. coli* as detailed in Fig. 2*A*. (*D*) Expression of *Arg1* and *Klf4* was measured by qPCR from WT or BCAP$^{-/-}$ BMDMs treated as in *C* in the presence or absence of 25 mM NaLa. Normalized to *Hprt1*. Data are representative of three independent experiments. Error bars represent SEM and Student *t* test was performed. *$P < 0.05$, **$P < 0.01$, ns, not significant.

requirement for BCAP in steady-state versus inducible histone lactylation. Inducible histone lactylation, however, is more involved during reparative macrophage transition (26). Understanding the precise relationship between lactate presence and histone lactylation at steady state and its contribution to macrophage biology will require further investigation.

Many mechanisms exist for dampening potentially tissue-injuring inflammation, including posttranslational modifications and inhibitory secreted factors (29–32). A major method by which TLR signaling intrinsically limits itself is through its simultaneous activation of the PI3K-AKT pathway (34). Chemical inhibition or genetic ablation of PI3K or AKT has been shown to enhance the secretion of inflammatory cytokines (37, 71). Activated PI3K phosphorylates AKT, which further inhibits its downstream targets GSK3β and FOXO1 (37, 38, 54, 55). As GSK3β and FOXO1 enhance NF-κB nuclear function, their phosphorylation and inhibition by AKT leads to a decrease in NF-κB–dependent transcription of inflammatory effectors (37, 38). Here we shown that BCAP$^{-/-}$ macrophages have sustained activation of GSK3β and FOXO1, therefore continually produce inflammatory cytokines. Chemical inhibition of GSK3β and FOXO1 reduced this prolonged activation of NF-κB and decreased levels of secreted IL-6 and IL-12. This is consistent with previous reports for the role of AKT signaling in macrophages, where the genetic ablation of this protein leads to an increase in the production of inflammatory effectors (71–73). Interestingly, even though inhibition of GSK3β and FOXO1 reduced production of inflammatory cytokines by BCAP$^{-/-}$ macrophages, it did not rescue their defect in undergoing the reparative macrophage transition. Our data verify that BCAP links TLR signaling to the PI3K-AKT-GSK3β-FOXO1 pathway as a means to negatively regulate inflammation, yet this is independent of its role in promoting the reparative transition of macrophages (Fig. 5). Our data unequivocally demonstrate that reparative transition is mechanistically uncoupled from dampening of the inflammation and that the metabolic product of aerobic glycolysis is critical for causing epigenetic changes that promote expression of tissue-repair genes (Fig. 5). Dampening inflammation is therefore not sufficient to initiate repair.

While we focus here on the intrinsic negative regulation that exists downstream of TLR signaling and find that it is sufficient for macrophages to undergo reparative transition, it is important to note that "alternatively activated" or reparative macrophages can also result from the presence of exogenous cytokines, like IL-4 and TGF-β (3, 8, 74). These cytokines influence macrophages to behave in an immune-suppressive manner, which is important during wound repair (3). Some markers for these wound-repair macrophages are *Arg1* and *Klf4*, which we also found to be upregulated in our in vitro macrophages following reparative transition. It is intriguing that TLR ligation, in a BCAP-dependent manner, and canonical macrophage alternative activation share common downstream features, and underscores the robustness of macrophage plasticity to respond to its environment. Taken together, the findings in this study helps to better understand both the regulation of reparative macrophage transition following TLR ligation and the modifications that control macrophage behavior during pathogen sensing. The ability for BCAP to be the upstream modulator of the TLR induced the PI3K-AKT pathway poises BCAP as a possible pharmacological target to modulate reparative macrophage transition in circumstances where either an inflammatory or antiinflammatory response is highly needed, such as in wound repair and autoinflammatory diseases.

Materials and Methods

Mice. C57BL/6 mice were purchased from Jackson Laboratory or from the University of Texas Southwestern Mouse Breeding Core Facility. BCAP$^{-/-}$ mice were previously generated (75) and were a gift from T. Kurosaki, Laboratory for Lymphocyte Differentiation, RIKEN Center for Integrative Medical Sciences (IMS-RCAI), Kanagawa, Japan, and Laboratory for Lymphocyte Differentiation, WPI Immunology Frontier Research Center, Osaka University, Osaka, Japan (39). BCAP$^{fl/fl}$ mice were previously generated by the University of Texas Southwestern Transgenic Core and published by Deason et.al. (45). LyzM Cre transgenic mice (obtained from Jackson Laboratory) were crossed to BCAP$^{fl/fl}$ mice to generate mice that specifically lack BCAP in macrophages (BCAP$^{\Delta M\phi}$ mice). BCAP$^{fl/fl}$ littermates were used as controls for all experiments

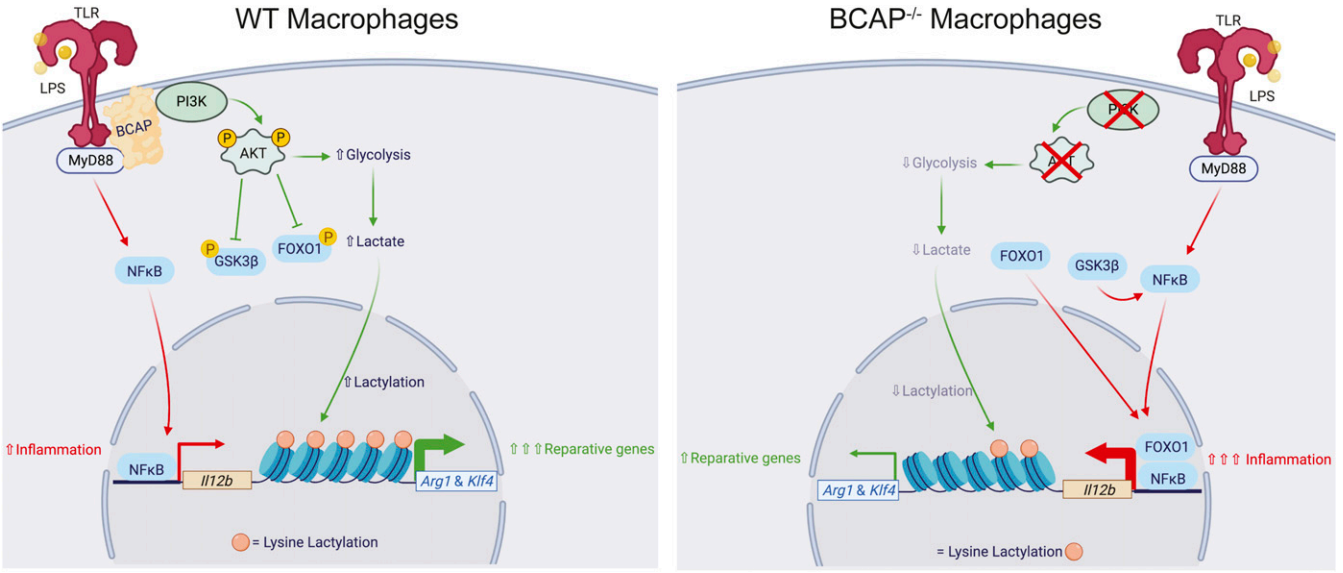

Fig. 5. Schematic representation of dual role of BCAP in regulating inflammatory responses and induction of tissue repair genes. (*Left*) In WT macrophages, TLR ligation by LPS leads to activation of NF-κB which culminates in production of inflammatory cytokines. TLR ligation also activates PI3K-AKT in a BCAP-dependent manner. Activated AKT phosphorylates its downstream targets FOXO1 and GSK3β to limit inflammation. AKT activation also enhances glycolysis, which leads to accumulation of metabolic byproducts like lactate. This metabolite is used to promote histone lactylation, which is important for the up-regulation of reparative genes and overall reparative transition of macrophages. (*Right*) In BCAP-deficient macrophages, TLR ligation does not lead to activation of the PI3K-AKT pathway, which results in lack of inactivation of FOXO1 and GSK3β resulting in enhanced inflammatory phenotype. In addition, lack of active AKT leads to decreased glycolysis and lower production of lactate. This translates into reduced histone lactylation and hampered expression of reparative genes, thus diminishing reparative macrophage transition. Figure was created using Biorender.

with BCAP$^{\Delta M\phi}$ mice. Mice used were between 6 and 12 wk of age and were maintained in specific pathogen-free conditions. All mouse experiments were done following approved protocols by the Institutional Animal Care and Use Committee at the University of Texas Southwestern Medical Center and Cincinnati Children's Hospital Medical Center.

DSS Colitis Model. Cohoused and age-matched BCAP$^{fl/fl}$ and BCAP$^{\Delta M\phi}$ mice were treated for 9 d with 2.5% 26 to 50 kDa DSS (MP Biomedicals) ad libitum in their drinking water. Weight was monitored daily. After 9 d, mice were killed and colons were carefully harvested from the cecum to the rectum. These colons were later used for histology, isolation of LP lymphocytes (LPLs), and qPCR. For the repair model, cohoused and age-matched BCAP$^{fl/fl}$ and BCAP$^{\Delta M\phi}$ mice were treated for 7 d with 2.5% 26 to 50 kDa DSS (MP Biomedicals) ad libitum in their drinking water. At day 7, DSS was removed and replaced with regular water for 9 subsequent days. For the survival study, the mice were checked each day for signs of morbidity, and their body weights were recorded. Survival was assessed as an indication of repair. Mice were killed when they exhibited the maximum loss of body weight. For some experiments, mice were killed before death to assess their colon length, gene expression, and to take sections for histology.

Histology. Mice were killed at indicated time points and colons were carefully harvested. Colons were rolled into Swiss rolls and fixed in 10% neutral-buffered formalin for 36 h, then submitted to the University of Texas Southwestern Molecular Pathology Core for tissue embedding and H&E staining. Slides were imaged at 10× or 20× using a DM2000 Compound Research Photomicroscope (Leica). Colon tissues from DSS colitis experiments were scored in a double-blinded fashion by the following parameters: Severity of inflammation (0–3), depth of injury/inflammation (0–3), and crypt damage (0–4). DSS histological scores were multiplied by a factor representing the percentage of tissue involvement: ×1 (0–25%), ×2 (26–50%), ×3 (51–75%), and ×4 (76–100%). Thus, the maximum colitis score in the DSS model is 40 (76).

Isolation of LPLs. LPLs were isolated as previously described (77, 78). In brief, intestines were carefully removed from mice and extensively washed using ice-cold PBS. Intestinal tissue was cut longitudinally, and then into ∼1-inch pieces. Tissues were incubated in 1 mM EDTA with rotation for removal of the epithelial cell layer. Tissues were further digested three times using Collagenase Type IV (Sigma-Aldrich) and DNase1 (Sigma-Aldrich), passed through a 40-μm filter, and subjected to a 40 to 70% Percoll gradient while centrifuged at 800 × *g* at room temperature for 20 min with centrifuge break at zero and using a slow acceleration. Neutrophils were isolated as described above but subjected to a 40 to 72 to 86% Percoll gradient. Lymphocytes and neutrophils were collected from the Percoll gradient and used for further analysis.

Flow Cytometry. FACS antibodies used for flow cytometry were Ly6C-BV711, Ly6G-FITC, CD11b-BV785, CD206-AF700, all obtained from BioLegend. For surface marker staining, cells were blocked with Fc Shield (anti-mouse CD16/CD32, Tonbo) for 10 min then incubated with surface antibodies for 30 min. Cells were extensively washed with FACS buffer (PBS, 2% FCS, and 2 mM EDTA). Samples were analyzed using Novocyte 3001 (ACEA Biosciences). Cells were gated on singlets, and dead cells were excluded using Zombie yellow live/dead staining (BioLegend). Data were analyzed using FlowJo software (BD).

Quantitative Real-Time PCR. Cells were collected and washed with PBS then lysed with TRIzol Reagent (Invitrogen). RNA was isolated with chloroform extraction and cDNA was synthesized using M-MLV reverse transcription (Invitrogen). qRT-PCR was performed using SYBR Green MasterMix (Applied Biosystems) and measured using QuantStudio 7 Flex Real-Time PCR System. Data were normalized to *Hprt1* levels within each sample. Primers used in this study are the following: *Il12b*-F (5′-GGTGTAACCAGAAAGGTGCG-3′), *Il12b*-R (5′-TTGGGGGACTCTTCCATCCT-3′), *Arg1*-F (5′-CTGACCTATGTGTCATTTGG-3′), *Arg1*-R (5′-CATCTGGGAACTTTCCTTTC-3′), *Klf4*-F (5′-CCCCTCTCCCATTATCAAG-3′), *Klf4*-R (5′-CTCTTGGTATAGGTTTTGCC-3′), *Hk2*-F (5′-GGGCTAGGAGCTACCACACA-3′), *Hk2*-R (5′-GGTCCAGAGCCAGGAACTC-3′), *Ldha*-F (5′-GAGTGGTGTGAATGTTGCCG-3′), *Ldha*-R (5′-CACCTCGTAGGCACTGTCCA-3′), *Ly6g*-F (5′-GAGAGGAAGTTTTATCTGTGCAGCC-3′), *Ly6g*-R (5′TCAGGTGGGACCCCAATACA-3′), *Cxcl1*-F (5′-CTGCACCCAAACCGAAGTCAT 3′), *Cxcl1*-R (5′-TTGTCAGAAGCCAGCGTTCAC-3′), *Mrc1*-F (5′-AAATGATGAGCTGTGGATTG-3′), *Mrc1*-R (5′-CCATCCTTGCCTTTCATAAC-3′)Hprt1-F (5′-CAGTCCCAGCGTCGTGATTA-3′), *Hprt1*-R (5′-TGGCCTCCCATCTCCTTCAT-3′), *Mmp9*-F (5′-CAGCCGACTTTTGTGGTCTTC-3′), *Mmp9*-R (5′-GTACAAGTATGCCTCTGCCA-3′).

BMDMs and Cell Culture. BMDMs were isolated and cultured using standard techniques. Briefly, femur and tibia were harvested, and bone marrow cells were isolated. Following RBC lysis, cells were cultured overnight in a tissue culture treated plate to remove stomal cells. Nonadherent cells were

collected and 4×10^6 cells/8 mL media were culture for 5 d in a nontreated Petri dish. Complete RPMI media (RPMI1640, L-glutamine, penicillin-streptomycin, sodium pyruvate, β-mercaptoethanol, 10% FCS) containing 30% L929 culture supernatant was used throughout. After differentiation, BMDMs were collected following removal of media and a brief incubation with ice cold PBS containing 2 mM EDTA, then plated for experiments.

For FOXO1 and GSK3β inhibition experiments, BMDMs were pretreated for 1 h with 1 μM SB216763 (Selleckchem), 1 μM AS1842856 (Selleckchem), or 10 mM LiCl (Sigma-Aldrich). BMDMs were then pulsed with LPS for 3 h in the presence of the inhibitors, then washed off and replaced with fresh media.

For exogenous lactate experiments BMDMs were pretreated with 25 mM NaLa (Sigma-Aldrich) for 1 h. Following pretreatment, cells were pulsed with LPS for 3 h. After pulse LPS was washed off and replaced with fresh supplemented with 25 mM NaLa.

HK *E. coli*. DH5α *E. coli* was grown to log-phase and measured at OD_{600} (OD_{600} 1.0 = 5×10^8 CFU). Bacteria were washed 3× with plain PBS and heat killed by incubating at 65 °C for 30 min. Bacteria were plated on an antibiotic-free plate overnight to confirm HK.

Western Blotting. Cells were washed twice with PBS and lysed with RIPA buffer containing protease inhibitor. Protein concentrations were quantified using the BCA Assay (Thermo Fisher Scientific), and equal amounts of protein were resolved on 4 to 12% Bis-Tris Plus gels (Thermo Fisher Scientific), transferred to PVDF membrane (EMD Millipore), and blocked with either 5% BSA for phospho-antibodies or 5% nonfat milk for the rest of antibodies. Primary antibodies used were obtained from Cell Signaling Technologies: pAKT (S473; (#4060), pGSK3b (S9; #5558), pFOXO1 (S256; #9461), total AKT (#4691), total GSK3β (12456), total FOXO1 (#2880), total H3 (#4499). PanKLa (PTM-1401) antibody was obtained from PTM biolabs. Blots were then probed with appropriate secondary antibodies conjugated to HRP (Bio-Rad) and developed using West pico plus ECL substrate (Thermo Fisher Scientific).

ELISA. Briefly, IL-12p40 or IL-6 coating antibody was diluted and incubated in a flat-bottom 96-well plate overnight at 4 °C, then blocked with PBS containing 1% BSA (Sigma-Aldrich) for 2 h. Samples were loaded in duplicate, diluted in blocking buffer, and incubated overnight. Detection antibodies were diluted and used according to manufacturer's instructions. Protein concentrations were quantified using *o*-phenylenediamine dihydrochloride colorimetric assay. Plates were washed extensively between steps with PBS and 0.05% Tween-20.

Seahorse and Lactate Assay. For the Seahorse assay, BMDMs from WT or BCAP KO mice were plated at a density of 80,000 cells per well in a seahorse 96-well plate (Agilent). Cells were pulsed with LPS 100 ng/mL (Sigma) or HK *E. coli* (multiplicity of infection [MOI] 100) and analyzed using the glycolysis stress test (10 mM glucose, 1 μM oligomycin, and 50 mM 2DG) by the Seahorse Extracellular Flux Analyzer (Agilent). To determine lactate production, BMDMs from WT or BCAP KO mice were pulsed with LPS 100 ng/mL (Sigma) or HK *E. coli* (MOI 100), as previously described. Supernatants were collected at the indicated time points, and lactate was measured using the BioVision Lactate Assay kit II.

Acid Extraction of Histones. Histones were extracted as previously described by Schechter et al. (79). Briefly, BCAP KO and WT BMDMs were pulsed with LPS (100 ng/mL) or HK *E. coli* (MOI 100) for indicated time points. Cell were then harvested and washed with ice-cold PBS. Cells were resuspended in a hypotonic lysis buffer and lysed for 30 min at 4 °C with rotation. Cells were then centrifuged at 10,000 × *g* for 10 min at 4 °C to pellet the intact nuclei. After centrifugation, nuclei were resuspended in 400 μL of 0.4 N H_2SO_4, and incubated overnight at 4 °C while rotating. Nuclei was then spun down at 16,000 × *g* for 10 min at 4 °C and the supernatant was moved to a new tube. TCA precipitation of histones was then performed using a final concentration of 33% TCA. Histones were then resuspended in ddH_2O and quantified using Micro BCA Assay (Thermo Fisher Scientific) and resolved normally.

Quantification and Statistical Analysis. Statistical analyses were performed in Prism (Graphpad) using unpaired or paired Student's *t* test as indicated in the figure legends. For survival curve, the statistics were performed using the log-rank test. Data are presented as mean ± SEM. Significance was considered at $*P < 0.05$, $**P < 0.01$, $***P < 0.001$, $****P < 0.0001$; ns, not significant.

Data Availability. All study data are included in the article and supporting information.

ACKNOWLEDGMENTS. We thank all the members of the C.P. laboratory for their insight, helpful discussions, and critical reading of this manuscript; Lisa Waggoner for maintaining the mouse colony and ensuring proper functioning of the laboratory; and Yajing Gao for critical reading of this manuscript. This work was supported by NIH Grants AI113125, AI123176, and GM120196 (to C.P.).

1. T. A. Wynn, A. Chawla, J. W. Pollard, Macrophage biology in development, homeostasis and disease. *Nature* **496**, 445–455 (2013).
2. J. W. Pollard, Trophic macrophages in development and disease. *Nat. Rev. Immunol.* **9**, 259–270 (2009).
3. P. J. Murray, Macrophage polarization. *Annu. Rev. Physiol.* **79**, 541–566 (2017).
4. P. J. Murray, T. A. Wynn, Protective and pathogenic functions of macrophage subsets. *Nat. Rev. Immunol.* **11**, 723–737 (2011).
5. C. F. Nathan, H. W. Murray, M. E. Wiebe, B. Y. Rubin, Identification of interferon-gamma as the lymphokine that activates human macrophage oxidative metabolism and antimicrobial activity. *J. Exp. Med.* **158**, 670–689 (1983).
6. T. Krausgruber *et al*., IRF5 promotes inflammatory macrophage polarization and TH1-TH17 responses. *Nat. Immunol.* **12**, 231–238 (2011).
7. S. Watanabe, M. Alexander, A. V. Misharin, G. R. S. Budinger, The role of macrophages in the resolution of inflammation. *J. Clin. Invest.* **129**, 2619–2628 (2019).
8. M. Stein, S. Keshav, N. Harris, S. Gordon, Interleukin 4 potently enhances murine macrophage mannose receptor activity: A marker of alternative immunologic macrophage activation. *J. Exp. Med.* **176**, 287–292 (1992).
9. F. O. Martinez *et al*., Genetic programs expressed in resting and IL-4 alternatively activated mouse and human macrophages: Similarities and differences. *Blood* **121**, e57–e69 (2013).
10. M. Hesse *et al*., Differential regulation of nitric oxide synthase-2 and arginase-1 by type 1/type 2 cytokines in vivo: Granulomatous pathology is shaped by the pattern of L-arginine metabolism. *J. Immunol.* **167**, 6533–6544 (2001).
11. X. Liao *et al*., Krüppel-like factor 4 regulates macrophage polarization. *J. Clin. Invest.* **121**, 2736–2749 (2011).
12. K. A. Wijnands *et al*., Arginase-1 deficiency regulates arginine concentrations and NOS2-mediated NO production during endotoxemia. *PLoS One* **9**, e86135 (2014).
13. N. Kapoor *et al*., Transcription factors STAT6 and KLF4 implement macrophage polarization via the dual catalytic powers of MCPIP. *J. Immunol.* **194**, 6011–6023 (2015).
14. J. Khallou-Laschet *et al*., Macrophage plasticity in experimental atherosclerosis. *PLoS One* **5**, e8852 (2010).
15. S. Tsimikas, Y. I. Miller, Oxidative modification of lipoproteins: Mechanisms, role in inflammation and potential clinical applications in cardiovascular disease. *Curr. Pharm. Des.* **17**, 27–37 (2011).
16. B. Vandanmagsar *et al*., The NLRP3 inflammasome instigates obesity-induced inflammation and insulin resistance. *Nat. Med.* **17**, 179–188 (2011).
17. J. M. Olefsky, C. K. Glass, Macrophages, inflammation, and insulin resistance. *Annu. Rev. Physiol.* **72**, 219–246 (2010).
18. B. Z. Qian, J. W. Pollard, Macrophage diversity enhances tumor progression and metastasis. *Cell* **141**, 39–51 (2010).
19. N. Kamada *et al*., Unique CD14 intestinal macrophages contribute to the pathogenesis of Crohn disease via IL-23/IFN-gamma axis. *J. Clin. Invest.* **118**, 2269–2280 (2008).
20. D. Bernardo *et al*., Human intestinal pro-inflammatory $CD11c^{high}CCR2^{+}CX3CR1^{+}$ macrophages, but not their tolerogenic $CD11c^{-}CCR2^{-}CX3CR1^{-}$ counterparts, are expanded in inflammatory bowel disease. *Mucosal Immunol.* **11**, 1114–1126 (2018).
21. Y. R. Na, M. Stakenborg, S. H. Seok, G. Matteoli, Macrophages in intestinal inflammation and resolution: A potential therapeutic target in IBD. *Nat. Rev. Gastroenterol. Hepatol.* **16**, 531–543 (2019).
22. O. R. Colegio *et al*., Functional polarization of tumour-associated macrophages by tumour-derived lactic acid. *Nature* **513**, 559–563 (2014).
23. A. Das *et al*., Monocyte and macrophage plasticity in tissue repair and regeneration. *Am. J. Pathol.* **185**, 2596–2606 (2015).
24. P. J. Murray *et al*., Macrophage activation and polarization: Nomenclature and experimental guidelines. *Immunity* **41**, 14–20 (2014).
25. F. Porcheray *et al*., Macrophage activation switching: An asset for the resolution of inflammation. *Clin. Exp. Immunol.* **142**, 481–489 (2005).
26. D. Zhang *et al*., Metabolic regulation of gene expression by histone lactylation. *Nature* **574**, 575–580 (2019).
27. K. A. Fitzgerald, J. C. Kagan, Toll-like receptors and the control of immunity. *Cell* **180**, 1044–1066 (2020).
28. R. Medzhitov, P. Preston-Hurlburt, C. A. Janeway Jr, A human homologue of the Drosophila Toll protein signals activation of adaptive immunity. *Nature* **388**, 394–397 (1997).
29. D. L. Boone *et al*., The ubiquitin-modifying enzyme A20 is required for termination of Toll-like receptor responses. *Nat. Immunol.* **5**, 1052–1060 (2004).
30. E. E. Turer *et al*., Homeostatic MyD88-dependent signals cause lethal inflamMation in the absence of A20. *J. Exp. Med.* **205**, 451–464 (2008).
31. D. Wald *et al*., SIGIRR, a negative regulator of Toll-like receptor-interleukin 1 receptor signaling. *Nat. Immunol.* **4**, 920–927 (2003).
32. K. Kobayashi *et al*., IRAK-M is a negative regulator of Toll-like receptor signaling. *Cell* **110**, 191–202 (2002).

33. T. Fukao *et al*., PI3K-mediated negative feedback regulation of IL-12 production in DCs. *Nat. Immunol.* **3**, 875–881 (2002).
34. M. Guha, N. Mackman, The phosphatidylinositol 3-kinase-Akt pathway limits lipopolysaccharide activation of signaling pathways and expression of inflammatory mediators in human monocytic cells. *J. Biol. Chem.* **277**, 32124–32132 (2002).
35. K. Hazeki, K. Nigorikawa, O. Hazeki, Role of phosphoinositide 3-kinase in innate immunity. *Biol. Pharm. Bull.* **30**, 1617–1623 (2007).
36. R. Katso *et al*., Cellular function of phosphoinositide 3-kinases: Implications for development, homeostasis, and cancer. *Annu. Rev. Cell Dev. Biol.* **17**, 615–675 (2001).
37. M. Martin, K. Rehani, R. S. Jope, S. M. Michalek, Toll-like receptor-mediated cytokine production is differentially regulated by glycogen synthase kinase 3. *Nat. Immunol.* **6**, 777–784 (2005).
38. W. Fan *et al*., FoxO1 regulates Tlr4 inflammatory pathway signalling in macrophages. *EMBO J.* **29**, 4223–4236 (2010).
39. T. D. Troutman *et al*., Role for B-cell adapter for PI3K (BCAP) as a signaling adapter linking Toll-like receptors (TLRs) to serine/threonine kinases PI3K/Akt. *Proc. Natl. Acad. Sci. U.S.A.* **109**, 273–278 (2012).
40. M. Ni *et al*., B-cell adaptor for PI3K (BCAP) negatively regulates Toll-like receptor signaling through activation of PI3K. *Proc. Natl. Acad. Sci. U.S.A.* **109**, 267–272 (2012).
41. T. Matsumura *et al*., Identification of BCAP-(L) as a negative regulator of the TLR signaling-induced production of IL-6 and IL-10 in macrophages by tyrosine phosphoproteomics. *Biochem. Biophys. Res. Commun.* **400**, 265–270 (2010).
42. O. Sharif, J. S. Brunner, A. Vogel, G. Schabbauer, Macrophage rewiring by nutrient associated PI3K dependent pathways. *Front. Immunol.* **10**, 2002 (2019).
43. C. M. Krawczyk *et al*., Toll-like receptor-induced changes in glycolytic metabolism regulate dendritic cell activation. *Blood* **115**, 4742–4749 (2010).
44. P. K. Langston, M. Shibata, T. Horng, Metabolism supports macrophage activation. *Front. Immunol.* **8**, 61 (2017).
45. K. Deason *et al*., BCAP links IL-1R to the PI3K-mTOR pathway and regulates pathogenic Th17 cell differentiation. *J. Exp. Med.* **215**, 2413–2428 (2018).
46. B. E. Clausen, C. Burkhardt, W. Reith, R. Renkawitz, I. Förster, Conditional gene targeting in macrophages and granulocytes using LysMcre mice. *Transgenic Res.* **8**, 265–277 (1999).
47. G. R. Jones *et al*., Dynamics of colon monocyte and macrophage activation during colitis. *Front. Immunol.* **9**, 2764 (2018).
48. T. A. Wynn, K. M. Vannella, Macrophages in tissue repair, regeneration, and fibrosis. *Immunity* **44**, 450–462 (2016).
49. K. L. Conway *et al*., p40phox expression regulates neutrophil recruitment and function during the resolution phase of intestinal inflammation. *J. Immunol.* **189**, 3631–3640 (2012).
50. K. L. Williams *et al*., Enhanced survival and mucosal repair after dextran sodium sulfate-induced colitis in transgenic mice that overexpress growth hormone. *Gastroenterology* **120**, 925–937 (2001).
51. J. F. Burgueño *et al*., Fluid supplementation accelerates epithelial repair during chemical colitis. *PLoS One* **14**, e0215387 (2019).
52. H. V. Groesdonk, S. Schlottmann, F. Richter, M. Georgieff, U. Senftleben, Escherichia coli prevents phagocytosis-induced death of macrophages via classical NF-kappaB signaling, a link to T-cell activation. *Infect. Immun.* **74**, 5989–6000 (2006).
53. R. G. Scheraga *et al*., TRPV4 mechanosensitive ion channel regulates lipopolysaccharide-stimulated macrophage phagocytosis. *J. Immunol.* **196**, 428–436 (2016).
54. M. Saline *et al*., AMPK and AKT protein kinases hierarchically phosphorylate the N-terminus of the FOXO1 transcription factor, modulating interactions with 14-3-3 proteins. *J. Biol. Chem.* **294**, 13106–13116 (2019).
55. D. A. Cross, D. R. Alessi, P. Cohen, M. Andjelkovich, B. A. Hemmings, Inhibition of glycogen synthase kinase-3 by insulin mediated by protein kinase B. *Nature* **378**, 785–789 (1995).
56. W. J. Ryves, A. J. Harwood, Lithium inhibits glycogen synthase kinase-3 by competition for magnesium. *Biochem. Biophys. Res. Commun.* **280**, 720–725 (2001).
57. B. Kelly, L. A. O'Neill, Metabolic reprogramming in macrophages and dendritic cells in innate immunity. *Cell Res.* **25**, 771–784 (2015).
58. V. R. Fantin, J. St-Pierre, P. Leder, Attenuation of LDH-A expression uncovers a link between glycolysis, mitochondrial physiology, and tumor maintenance. *Cancer Cell* **9**, 425–434 (2006).
59. B. Everts *et al*., TLR-driven early glycolytic reprogramming via the kinases TBK1-IKKε supports the anabolic demands of dendritic cell activation. *Nat. Immunol.* **15**, 323–332 (2014).
60. M. G. Vander Heiden, L. C. Cantley, C. B. Thompson, Understanding the Warburg effect: The metabolic requirements of cell proliferation. *Science* **324**, 1029–1033 (2009).
61. S. E. Corcoran, L. A. O'Neill, HIF1α and metabolic reprogramming in inflammation. *J. Clin. Invest.* **126**, 3699–3707 (2016).
62. J. Fan, K. A. Krautkramer, J. L. Feldman, J. M. Denu, Metabolic regulation of histone post-translational modifications. *ACS Chem. Biol.* **10**, 95–108 (2015).
63. X. Su, K. E. Wellen, J. D. Rabinowitz, Metabolic control of methylation and acetylation. *Curr. Opin. Chem. Biol.* **30**, 52–60 (2016).
64. M. A. Reid, Z. Dai, J. W. Locasale, The impact of cellular metabolism on chromatin dynamics and epigenetics. *Nat. Cell Biol.* **19**, 1298–1306 (2017).
65. M. A. Akbar *et al*., ARC syndrome-linked Vps33B protein is required for inflammatory endosomal maturation and signal termination. *Immunity* **45**, 267–279 (2016).
66. S. Greenberg, S. Grinstein, Phagocytosis and innate immunity. *Curr. Opin. Immunol.* **14**, 136–145 (2002).
67. A. K. Jha *et al*., Network integration of parallel metabolic and transcriptional data reveals metabolic modules that regulate macrophage polarization. *Immunity* **42**, 419–430 (2015).
68. J. S. Moon *et al*., UCP2-induced fatty acid synthase promotes NLRP3 inflammasome activation during sepsis. *J. Clin. Invest.* **125**, 665–680 (2015).
69. J. Ecker *et al*., Induction of fatty acid synthesis is a key requirement for phagocytic differentiation of human monocytes. *Proc. Natl. Acad. Sci. U.S.A.* **107**, 7817–7822 (2010).
70. L. A. O'Neill, R. J. Kishton, J. Rathmell, A guide to immunometabolism for immunologists. *Nat. Rev. Immunol.* **16**, 553–565 (2016).
71. A. Arranz *et al*., Akt1 and Akt2 protein kinases differentially contribute to macrophage polarization. *Proc. Natl. Acad. Sci. U.S.A.* **109**, 9517–9522 (2012).
72. E. Vergadi, E. Ieronymaki, K. Lyroni, K. Vaporidi, C. Tsatsanis, Akt signaling pathway in macrophage activation and M1/M2 polarization. *J. Immunol.* **198**, 1006–1014 (2017).
73. A. Androulidaki *et al*., The kinase Akt1 controls macrophage response to lipopolysaccharide by regulating microRNAs. *Immunity* **31**, 220–231 (2009).
74. S. Gordon, F. O. Martinez, Alternative activation of macrophages: Mechanism and functions. *Immunity* **32**, 593–604 (2010).
75. T. Yamazaki *et al*., Essential immunoregulatory role for BCAP in B cell development and function. *J. Exp. Med.* **195**, 535–545 (2002).
76. C. F. Krieglstein *et al*., Role of blood- and tissue-associated inducible nitric-oxide synthase in colonic inflammation. *Am. J. Pathol.* **170**, 490–496 (2007).
77. I. I. Ivanov *et al*., The orphan nuclear receptor RORgammat directs the differentiation program of proinflammatory IL-17+ T helper cells. *Cell* **126**, 1121–1133 (2006).
78. W. Hu, T. D. Troutman, R. Edukulla, C. Pasare, Priming microenvironments dictate cytokine requirements for T helper-17 cell lineage commitment. *Immunity* **35**, 1010–1022 (2011).
79. D. Shechter, H. L. Dormann, C. D. Allis, S. B. Hake, Extraction, purification and analysis of histones. *Nat. Protoc.* **2**, 1445–1457 (2007).